



Android-based wireless single-lead electrocardiogram: heart rate measurement and ECG signal visualization

Atika Novitasari¹, Nuryani Nuryani^{*1}, Darsono Darsono¹

Universitas Sebelas Maret, Surakarta, Indonesia¹

Article Info

Keywords:

Heart Rate, Android, Electrocardiogram, Pan-Tompkins, Single Lead

Article history:

Received: December 29, 2023

Accepted: June 09, 2024

Published: August 31, 2024

Cite:

A. Novitasari, N. Nuryani, and D. Darsono, "Android-Based Wireless Single-Lead Electrocardiogram: Heart Rate Measurement and ECG Signal Visualization", KINETIK, vol. 9, no. 3, Jul. 2024.
<https://doi.org/10.22219/kinetik.v9i3.1943>

*Corresponding author.

Nuryani Nuryani

E-mail address:

nuryani@mipa.uns.ac.id

Abstract

Heart rate (HR) is vital for medical and healthcare purposes. This study presents an Android-based heart rate measurement system utilizing a single-lead electrocardiogram (ECG). Three electrodes placed on the arm in lead I configuration capture the ECG signals. An AD8232 sensor amplifies the signal, which is then digitized by Arduino Nano and transmitted to an Android device via HC-05 Bluetooth. The Android application processes the ECG data using the Pan-Tompkins algorithm with an optimized threshold coefficient to extract HR information. The system displays the ECG waveform and the calculated HR on the user interface. Our evaluation demonstrates high accuracy with an error rate of only 0.042%, sensitivity of 99.84%, and positive predictive value of 97.06%. This research suggests the potential of this system for convenient and reliable HR monitoring using readily available smartphones.

1. Introduction

Heart rate (HR) is vital for medical and healthcare purposes. A medical instrument that can record heart signals and measure the HR through electrodes placed on the skin is called an electrocardiograph (ECG). Recording heart signals using ECG is a gold standard for some reasons, i.e., it is an inexpensive instrument, it has varied signal parameters, and it is non-invasive [1]. ECG signal recordings obtained by electrodes on the skin itself can represent cardiac polarization and depolarization [2]. The placement of ECG electrodes affects the generated signal. A standard 12-lead ECG provides the highest resolution with ten electrodes placed on the patient's chest, legs, and arms. Electrodes placement in this position is complex and cannot be used without medical supervision [3]. Therefore, it is necessary to use a portable and easy-to-use ECG, namely ECG single lead with two electrodes placed on the arms [4].

ECG recording consists of the important signal parameters representing the cardiovascular system phase, such as P, Q, R, S, and T waves, RR interval, ST segment, and QRS complex. For calculating HR, the quality of R-peak is important. R-peak signal can be obtained by detecting the QRS complex [5]. Two of the most commonly used algorithms for QRS complex detection are the Pan-Tompkins algorithm and Wavelets transform. Both algorithms can be combined; one recent research used Discrete Wavelets Transform (DWT) as the denoising algorithm and Pan-Tompkins as the QRS detection algorithm [6]. Pan-Tompkins algorithm is an easily adapted algorithm that uses an adaptive threshold to detect QRS signals accurately, even in bad signal conditions [7-13]. Research about Pan-Tompkins shows that accuracy, sensitivity, and positive prediction of QRS complex detection perform well even in noisy signals [14, 15].

Numerous researchers compared single-lead ECG to the other ECG lead placements. The study showed that single-lead ECG placement performs better than the other lead placements. Single-lead ECG, placed on the arm and leg, commonly combined with the Pan-Tompkins algorithm, showed good performance compared to the different algorithms [16-18].

The AD8232 is a little chip sensor used to measure the heart's electrical activity, particularly the ECG signal. Electrical activity of the heart is commonly extremely noisy, and the op-amp of the AD8232 sensor helps to obtain a clear signal from the PR and QT intervals [19]. The AD8232 sensor is commonly used as integrated signal conditioning for ECG and other bio-potential measurement [20]. This sensor is suitable for portable ECG since it is compact and easy to connect with other components.

The rise of sensor-equipped smartphones offers exciting mobile and user-friendly HR monitoring possibilities. This article delves into the state-of-the-art Android-based single-lead ECG HR monitoring systems. We will discuss the hardware requirement, signal acquisition techniques, processing algorithms, and the challenges associated with this approach.

This article introduces a heart rate measurement technique using a single-lead ECG with lead I placement on both arms. Compared to a traditional 12-lead ECG, this method offers significant advantages for practical heart rate (HR) monitoring. One major advantage is the convenience and ease of use; setting up the lead requires only two electrodes placed on the arms, making it significantly faster and simpler than a 3-lead or 12-lead ECG. This minimal setup can be done by individuals without medical expertise. Another advantage is the portability, as no additional equipment is required besides the electrodes and a device capable of reading the signal, potentially even a smartphone with a suitable app. This makes it ideal for use in remote locations or situations with limited access to conventional ECG equipment. Additionally, when positioned correctly, lead I can provide a relatively accurate measurement of heart rate, which proves valuable in scenarios requiring a quick HR assessment, such as during exercise routines, monitoring someone experiencing mild discomfort, or in emergencies with limited resources.

The following sections will present the research method in the second section, including the heart rate measurement system design and the Pan-Tompkins algorithm. This is followed by the third section, which presents the results and discussion. The conclusion is presented in the fourth section.

2. Research Method

2.1 Heart Rate Measurement System Design

System design in this study is divided into two categories, i.e., transmitter combined with recorder and receiver. The transmitter unit consists of an AD8232 ECG sensor as a bio-potential recorder, a microcontroller Arduino Nano as an analog-digital converter, and HC-05 Bluetooth as a wireless Bluetooth module. Figure 1 shows the heart rate measurement system design, consisting of three transmitter units and an android receiver unit. The receiver unit, Android interface, shows ECG graphs and heart rate (HR) values.

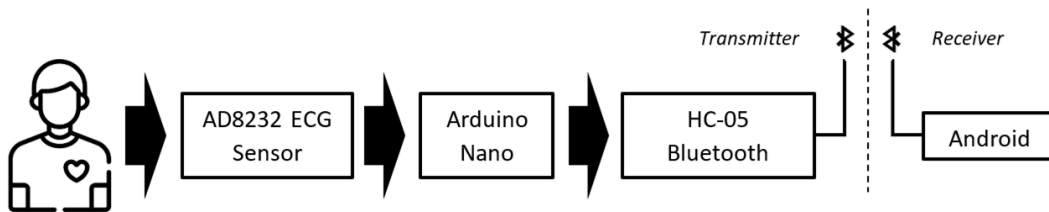


Figure 1. Heart Rate Measurement System Design

AD8232 sensor used three electrodes, i.e., red electrode labeled as R (right), yellow electrode labeled as L (left), and green electrode labeled as F (foot). Each electrode is connected with a different input, such as R connected with IN-, L connected with IN+, and L associated with a driven amplifier [21]. In this study, three electrodes were placed on the arm, with two electrodes, L and F, on the left and R on the right. This placement could represent lead I placement that used both arm bio-potential [22]. This study’s electrode placement and hardware diagram system, respectively, are shown in Figure 2 and Figure 3.

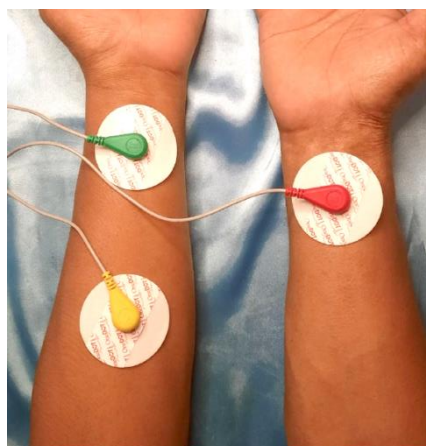


Figure 2. Electrodes Placement According to Lead I Position

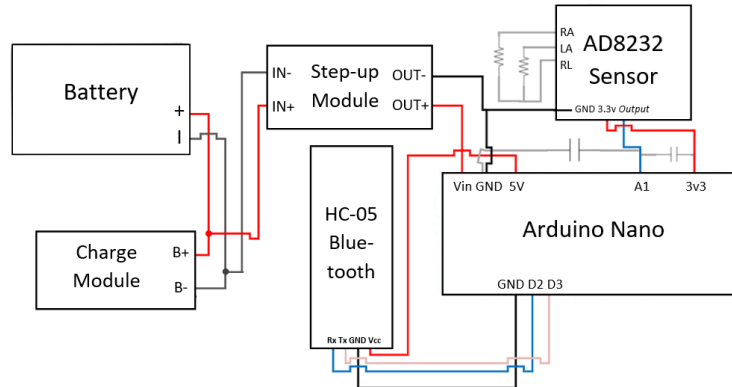


Figure 3. Wired Diagram of Heart Rate Measurement system

2.2 Pan-Tompkins Algorithm

For heart rate measurement, ECG parameters, specifically QRS complex and RR interval, are commonly used [23]. To detect these parameters, an adaptable algorithm like Pan-Tompkins is needed. Pan-Tompkins is a suitable algorithm that performs well in any ECG signal condition [6]. Generally, the Pan-Tompkins algorithm has five-step signal processing, i.e., filtering, derivative, squaring, moving window integration, and QRS complex detection [24]. The QRS complex detected by the Pan-Tompkins algorithm will be used to calculate the RR interval and HR value.

The proposed method used filtering as the first step. A range 5-15 Hz band-pass filter is used. This band-pass range is a common frequency of the QRS complex [14]. The next step is derivative, squaring, and moving window integration, which highlights the QRS complex, specifically R-peak. The last step is QRS complex detection with adaptive threshold. Equations 1 to 4 calculate the adaptive threshold [14, 24].

$$RPL = 0,125 PEAKI + 0,875 RPL \quad (1)$$

$$NPL = 0,125 PEAKI + 0,875 NPL \quad (2)$$

$$THRESHOLD1 = NPL + \alpha (RPL - NPL) \quad (3)$$

$$THRESHOLD2 = 0,5 THRESHOLD1 \quad (4)$$

Notation:

RPL	= R-peak level
NPL	= Noise peak level
$PEAKI$	= Peak level
α	= Threshold coefficient
$THRESHOLD1$	= First threshold
$THRESHOLD2$	= Second threshold

Detected R-peak used to calculate RR interval. Then, the RR interval was used to estimate HR with beats per minute (bpm) as the unit. Equation 5 shows the HR equation with MRR as the mean interval RR.

$$HR = \frac{60,000}{MRR} \quad (5)$$

2.3 Performance Evaluation

The proposed method has false detection possibilities. Three performances, i.e., error, sensitivity, and positive predictive, are used to evaluate the system. R-peak that the system has detected is used to calculate these three performances. Equations 6 to 8, respectively, are used to calculate error, sensitivity, and positive predictive value [25].

$$E (\%) = \frac{FP + FN}{TB} \times 100\% \quad (6)$$

$$S (\%) = \frac{TP}{TP + FN} \times 100\% \quad (7)$$

$$PP (\%) = \frac{TP}{TP + FP} \times 100\% \tag{8}$$

Notation

- E (%)* = Percent error
- S (%)* = Percent sensitivity
- PP (%)* = Percent positive predictive
- FP* = False positive
- FN* = False negative
- TP* = True positive
- TB* = Total R-peak detected

3. Results and Discussion

The hardware and display system are shown in Figure 4. The developed system used HC-05 Bluetooth as the wireless communication tool. The data from the AD8232 Sensor is transferred to Android through Bluetooth. The data was processed in an Android application and shown as ECG graphs and real-time Heart Rate (HR) values. The Android interface also displays the CSV file name, which stores the data and time stamps.

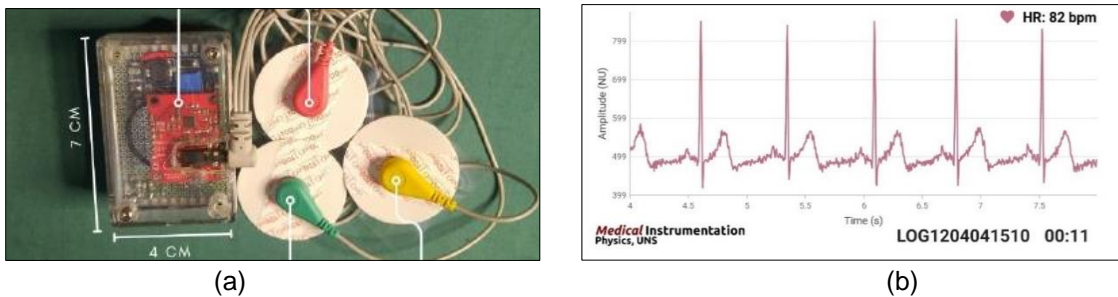


Figure 4. (a) Unit Overview and (b) Main Page

3.1 Pan-Tompkins ECG signal processing

The pan-Tompkins algorithm used in this study consists of five steps, i.e., filtering, derivative, moving window integration, and QRS complex detection [24]. The raw ECG signal is plotted in a graph shown in Figure 5.

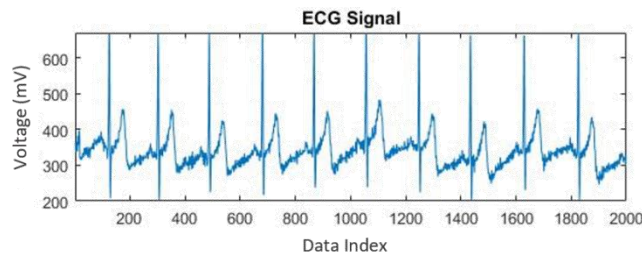


Figure 5. Raw ECG signal

Raw ECG signal is filtered with a band-pass filter to reduce noise. This system uses two cut-off frequencies, i.e., 5 Hz for the high pass filter and 15 Hz for the low pass filter. Figure 6 (a) shows the filtered ECG signal. Band-pass filtered ECG signal then faced derivative step. The derivative step aims to highlight the R-peak. Figure 6 (b) shows the result of the derivative step.

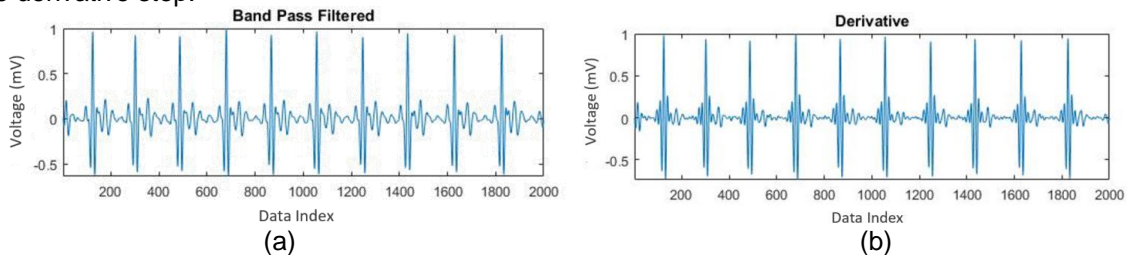


Figure 6. (a) Filtered ECG Signal (b) ECG Signal after Derivative Filtering

ECG signal that has sharp R-peak after derivative step then faced squaring step. This step squared all the data points to highlight the highest peak [26]. Figure 7 (a) shows the graph result after the squaring step. Moving window integration is the last step before QRS complex detection. The proposed method used 30 window length (150 ms) and 200 Hz sampling rate to align QRS reference points [24, 27]. Figure 7 (b) shows the ECG signal after the moving window integration step. After moving window integration, the QRS complex will be detected using the threshold method. Peaks that pass the threshold value will be detected as R peaks.

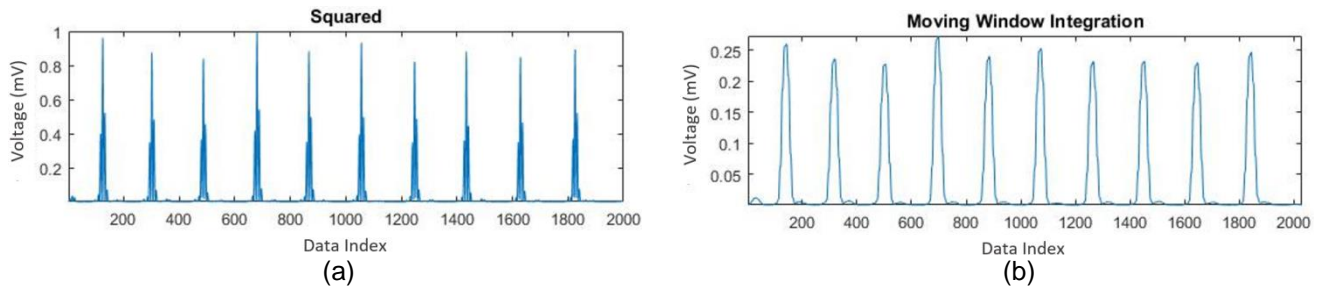


Figure 7. (a) Squared ECG Signal (b) ECG Signal after Moving Window Integration

3.2 QRS Complex Detection

This study used ten raw ECG data from 10 different patients. All of the patients are in a healthy and relaxed condition. The data were collected from the patient for 2 minutes, but in this process, the data will be fragmented into different lengths. Figure 8 (a) and (b) show the results of R-peaks detection using 0.05 as the threshold coefficient value. The figure shows two graphs, i.e., R-peaks detection on the signal after the moving window integration process (a) and R-peaks detection on the raw signal before Pan-Tompkins processing. After R-peaks have been detected, it will be used to calculate RR intervals. Mean of RR intervals will be used to estimate HR value using Equation 5.

Based on Liu et al. and Pan & Tompkins [14, 24], the standard threshold coefficient for the Pan-Tompkins method is 0.5. Hence, using 0.05 as the threshold coefficient, R-peaks detection also detected false positive R-peaks. Figure 8 shows two false positives detected from patient No. 001 fragmented signal. This fragmented signal has 8 seconds duration, 8000 data points, and 2/12 or 16,67% error R-peaks detection.

The different results were shown by Detecting R-peaks using 0.25 and 0.5 threshold coefficient values. Figure 9 (a) and (b) show the result of R-peaks detection from patient No. 001 using two different threshold coefficients, 0.25 and 0.5. The threshold coefficients used in 9 (a) and (b) have the same R-peaks detection results on patient No. 001 fragmented ECG signal. These data have 0% error since all detected peaks are true positive.

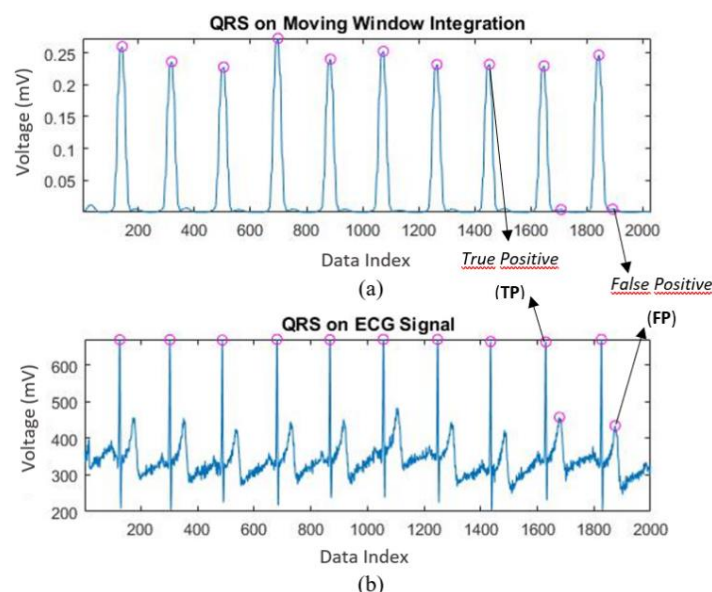


Figure 8. The Results of R-Peaks Detection from Patient No. 001 with 0.05 as the Threshold Coefficient Value on (a) Signal After Moving Window Integration, (b) Raw Signal

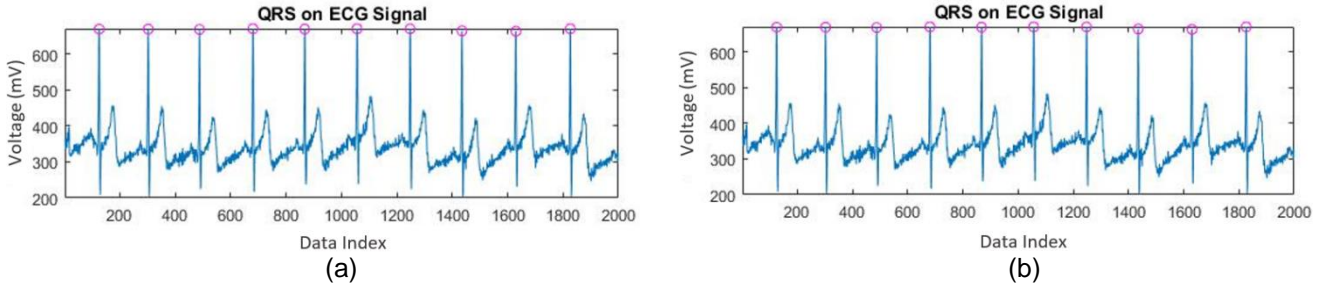


Figure 9. (a) The Result of R-Peaks Detection from Patient No. 001 with 0.25 and (b) 0.5 as the Threshold Coefficient

This study collected raw ECG data from 10 people between 18-50 years old. The data is transferred through a Bluetooth wireless connection. The raw data consists of two columns: time stamps with 0,05s intervals and voltage (mV). The average length of the raw data is 2 minutes, and then each is fragmented into 45 seconds, which consists of 9000 data points. All of the data is processed using three different threshold coefficients. The sum of R-peak detection results and performance calculation is shown in Table 1. TP means True Positive, FP means False Positive, and FN means False Negative—the performance calculation using Equations 6, 7, and 8.

Table 1. Accumulation of TP, FP, FN, and Performance Calculation

Threshold coefficient (α)	ΣPeaks Detection			E (%)	S (%)	PP (%)
	TP	FP	FN			
0.05	627	620	0	49.72	100	50.28
0.25	627	136	0	17.82	100	82.18
0.5	627	19	1	3.09	99.84	97.06

Table 1 shows different results of performance calculation. Threshold coefficients 0.05 and 0.25 have 100% sensitivity but have less performance results on peak detection error and positive predictive. As mentioned, the standard threshold coefficient is 0.05; the threshold coefficient under 0.5 has fewer performance results. The threshold coefficient of 0.5, the standard threshold coefficient, generated the best performance in this study, as shown in Table 1. Hence, for the next processing step, a threshold coefficient 0.5 is used to detect R-peaks using the Pan-Tompkins ECG detection method.

3.3 Heart Rate Measurement Result

The system has been tested. The performance is measured in terms of Error (E) in %, using Equation 6. Both HR, manual and by-system, generate values between 63-100 bpm (beats per minute). Table 2 shows the error values with a different sum of R-peaks. The heart rate measurement results were analyzed based on the number of ECG R-peaks used for calculation. The average error values for different sums of R-peaks indicate notable variations. For a sum of 4 R-peaks, the average error is 0.512%. When the sum of R-peaks is increased to 6, the average error significantly decreases to 0.055%. However, with 8 R-peaks, the average error rises again to 0.602%. When using 10 and 12 R-peaks, the average error values are very similar, at 0.042% and 0.043%, respectively.

These findings suggest that the lowest average error is achieved with 10 R-peaks, followed closely by 12 R-peaks, indicating that using a higher sum of R-peaks generally improves the accuracy of heart rate measurement. However, there is an optimal range beyond which the improvement in accuracy plateaus, as seen with the similar error values for 10 and 12 R-peaks. Interestingly, the average error is higher when using 8 R-peaks than 4 R-peaks. This anomaly might be attributed to variations in the ECG signal quality or other external factors affecting the measurement accuracy, warranting further investigation—these values align with the other papers [14,15].

In general, while increasing the sum of R-peaks generally enhances the accuracy of heart rate measurements, there is a point of diminishing returns. The results suggest that using ten or more R-peaks balances the measurement accuracy and computational efficiency.

$$E (\%) = \frac{|HR_{manual} - HR_{system}|}{HR_{manual}} \times 100\% \tag{6}$$

where:

- $E (\%)$ = Percent error
- HR_{manual} = Heart rate value calculated using visible R-peaks
- HR_{system} = Heart rate generated by the system

Table 2. The Average Error Value from each Sum of R-peaks

ΣR	Average E (%)
4	0.512
6	0.055
8	0.602
10	0.042
12	0.043

4. Conclusion

A study on the design of an Android-based heart rate measurement system using a single-lead electrocardiogram (ECG) with lead I placement has been conducted. The system employs the Pan-Tompkins algorithm and utilizes three electrodes placed according to the lead I position. The system's performance was evaluated based on certain threshold coefficients and the number of R-peaks used for calculation. The proposed design achieved an average error of 0.042%, a sensitivity of 99.84%, and a positive predictive value of 97.06%. The optimum combination that generated the best performance was a threshold coefficient of 0.5 and a sum of 10 R-peaks. Further research on ECG lead I using the Pan-Tompkins algorithm is necessary, particularly involving variations in the threshold coefficient and the number of R-peaks to enhance system performance and reliability.

Acknowledgment

This study was supported by the Institute of Research and Community Service, Lembaga Penelitian dan Pengabdian pada Masyarakat (LPPM), at Universitas Sebelas Maret (UNS), Indonesia.

References

- [1] Gilgen-Ammann, R., Schweizer, T., and Wyss, T., "RR Interval Signal Quality of A Heart Rate Monitor and An ECG Holter at Rest and During Exercise," *European Journal of Applied Physiology*, Vol. 119, No. 7, Pp. 1525-1532, 2019. <https://doi.org/10.1007/s00421-019-04142-5>
- [2] Marinho, L. B., Nascimento, N. de M. M., Souza, J. W. M., Gurgel, M. V., Reboucas Filho, P. P., and de Albuquerque, V. H. C., "A Novel Electrocardiogram Feature Extraction Approach for Cardiac Arrhythmia Classification," *Future Generation Computer System*, Vol. 97, Pp. 564-577, 2019. <https://doi.org/10.1016/j.future.2019.03.025>
- [3] Shaown, T., Hasan, I., Mim, M. M. R., and Hossain, M. S. H., "IoT-based Portable ECG Monitoring System for Smart Healthcare," in *1st International Conference on Advances in Science, Engineering and Robotics Technology (ICASERT)*, Pp. 1-5, 2019. <http://dx.doi.org/10.1109/ICASERT.2019.8934622>
- [4] Abdou, A. and Krishnan, S., "Horizons in Single-Lead ECG Analysis From Devices to Data", *Frontiers in Signal Processing*, Vol. 2, Pp. 1-16, 2022. <https://doi.org/10.3389/frsip.2022.866047>
- [5] Kranjec, J., Begus, S., Gersak, G., and Drnovsek, J., "Non-contact Heart Rate and Heart Rate Variability Measurements: A Review", *Biomedical Signal Processing and Control*, Vol. 13, Pp. 102-112, 2014. <https://doi.org/10.1016/j.bspc.2014.03.004>
- [6] Soe, Y. N. and Oo, K. K. K., "ECG Signal Classification using Discrete Wavelet Transform and Pan Tompkins Algorithm", *International Journal Of Creative and Innovative Research In All Studies*, Vol. 2, No. 11, Pp. 14-19, 2020.
- [7] Liu, Y., Chen, J., Bao, N. Gupta, B. B., and Lv, Z., "Survei on Atrial Fibrillation Detection from A Single-lead ECG Wave for Internet of Medical Things," *Computer Communications*, Vol. 178, Pp. 245-258, 2021. <http://dx.doi.org/10.1016/j.comcom.2021.08.002>
- [8] Rana, A. and Kim, K. K., "Cardiac Disease Detection Using Modified Pan-Tompkins Algorithm," *Journal of Sensor Science and Technology*, Vol. 28, No. 1, Pp. 13-16, 2019. <http://dx.doi.org/10.5369/JSST.2019.28.1.13>
- [9] Utomo, T. P., Nuryani, N., and Darmanto, "QRS Peak Detection for Heart Rate Monitoring on Android Smartphone," in *Journal of Physics: Conference Series*, Vol. 909, Pp. 1-7, 2017. <http://dx.doi.org/10.1088/1742-6596/909/1/012006>
- [10] Shokouejad, M., Chiang, M., Lines, S., Wang, F., Tompkins, W., and Webster, J. G., "Systematic Design and HRV Analysis of a Portable ECG System Using Arduino and LabVIEW for Biomedical Engineering Training," *International Journal of Electronics and Electrical Engineering*, Vol. 5, No. 5, Pp. 301-311, 2017. <http://dx.doi.org/10.18178/ijeee.5.5.301-311>
- [11] Utomo, T. P., Nuryani, N., and Nugroho, A. S., "Automatic QRS-complex Peak Detector Based on Moving Average and Thresholding," in *Journal of Physics: Conference Series*, Vol. 1153, Pp. 1-6, 2019. <http://dx.doi.org/10.1088/1742-6596/1153/1/012039>
- [12] Shalihah, A., Alhafid, F., Subekti, N. Y. S., Utomo, T.P., and Nuryani, N., "Electrocardiogram Monitoring System Based on Android Smartphone and Microcontroller Unit," in *Journal of Physics: Conference Series*, Vol. 1153, Pp. 1-5, 2017.
- [13] Abd Al-Jabbar, E. Y., Al-Hatab, M. M. M., Qasim, M. A., Fathel, W. R., and Fadhil, M. A., "Clinical Fusion for Real-Time Complex QRS Pattern Detection in Wearable ECG Using the Pan-Tompkins Algorithm", *Journal of Fusion: Practice and Applications*, Vol. 12, No. 2, Pp. 172-184, 2023. <https://dx.doi.org/10.54216/FPA.120214>
- [14] Liu, F., Wei, S., Li, Y., Jiang, X., Zhang, Z., Zhang, L., and Liu, C., "The Accuracy on the Common Pan-Tompkins Based QRS Detection Methods Through Low-Quality Electrocardiogram Database," *Journal of Medical Imaging and Health Informatics*, Vol. 7, Pp. 1-5, 2017. <http://dx.doi.org/10.1166/jmihi.2017.2134>
- [15] Fariha, M. A. Z., Ikeura, R., Hayakawa, S., and Tsutsumi, S., "Analysis of Pan-Tompkins Algorithm Performance with Noisy ECG Signals," in *Journal of Physics: Conference Series*, Vol. 1532, Pp. 1-11, 2020. <http://dx.doi.org/10.1088/1742-6596/1532/1/012022>
- [16] Vasudeva, S. T., Rao, S. S., Panambur, N. K., Shettigar, A. K., Mahabala, C., Chandrashekarappa, M. P. G., and Linul, E., "Development of A Convolutional Neural Network Model to Predict Coronary Artery Disease Based on Single-Lead and Twelve-Lead ECG Signals", *Applied Sciences*, Vol. 12, No. 15, Pp. 1-25, 2022. <https://doi.org/10.3390/app12157711>
- [17] Jimenez-Serrano, S., Rodrigo, M., Calvo, C. J., Millet, J., and Castells, F., "From 12 to 1 ECG Lead: Multiple Cardiac Condition Detection Mixing A Hybrid Machine Learning Approach with A One-versus-rest Classification Strategy", *Physiological Measurement*, Vol. 43, No. 6, Pp. 1-17, 2022. <http://dx.doi.org/10.1088/1361-6579/ac72f5>
- [18] Shokouejad, M., Mehdi Shokouejad, M.C., Chiang, M., Lines, S., Wang, F., Tompkins, W.J., and Webster, J.G., "Systematic Design and HRV Analysis of a Portable ECG System Using Arduino and LabVIEW for Biomedical Engineering Training", *International Journal of Electronics and Electrical Engineering*, Vol. 5, No. 5, Pp. 301-311, 2017. <http://dx.doi.org/10.18178/ijeee.5.5.301-311>

- [19] Chhabra, M., and Kalsi, M., "Real Time ECG monitoring system based on Internet of Things (IoT)", *International Journal of scientific and research publications*, Vol. 7, No. 8, Pp. 547-550, 2017.
- [20] Hamad, A. M., dan Jasim, A. D., "Remote ECG Signal Monitoring and Classification Based on Arduino with AD8232 Sensor", *University of Thi-Qar Journal for Engineering Sciences*, Vol. 11, No. 2, Pp. 95-101. [http://dx.doi.org/10.31663/tqujes.11.2.393\(2021\)](http://dx.doi.org/10.31663/tqujes.11.2.393(2021))
- [21] Analog Devices, "Single-lead Heart Rate Monitor Front End AD8232", in *Analog Devices*, Pp. 1-32, 2013.
- [22] Nguyen, L., Perry, R., Seneres, L., and Seyedm Mahmoud, N., "Analog Integrated Circuit Applications", in Faculty of the Worcester Polytechnic Institute, Pp. 1-131, 2015.
- [23] Tyagi, D. And Kumar R., "Identification of QRS Segments of Electrocardiogram Signals Using Feature Extraction", in *6th International Conference for Convergence in Technology I2CT*, Pp. 1-5, 2021. <http://dx.doi.org/10.1109/I2CT51068.2021.9417869>
- [24] Pan, J., and Tompkins, W. J., "A Real-Time QRS Detection Algorithm," *IEEE Transactional Biomedical Engineering*, Vol. BME-32, No. 3, Pp. 230-236, 1985. <https://doi.org/10.1109/TBME.1985.325532>
- [25] Neri, L., Oberdier, M. T., Augello, A., Suzuki, M., Tumarkin, E., Jaipalli, S., Geminiani, G. A., Halperin, H. R., and Borghi C., "Algorithm for Mobile Platform-Based Real-Time QRS Detection," *Sensors*, Vol. 23, No. 3., Pp. 1-9, 2023. <http://dx.doi.org/10.3390/s23031625>
- [26] Apandi, Z. F. M., Ikeura, R., Hayakawa, S., and Tsutsumi, S., "QRS Detection in Electrocardiogram Signal of Exercise Physical Activity," in *Journal of Physics: Conference Series*, Vol. 2319, No. 1, Pp. 1-9, 2022. <http://dx.doi.org/10.1088/1742-6596/2319/1/012021>
- [27] Urteaga, J., Elola, A., Aramendi, E., Norvik, E., and Skogvoll, E., "Automated Algorithm for QRS Detection in Cardiac Arrest Patients with PEA," *Computing in Cardiology*, Vol. 49, Pp. 3-6, 2022. <https://doi.org/10.22489/CinC.2022.270>